Acta Cryst E CRYSTALLOGRAPHIC COMMUNICATIONS

ISSN 2056-9890

Crystal structure of the acyclic form of 1-deoxy-1-[(4-methoxyphenyl)(methyl)amino]-D-fructose

Valeri V. Mossine,[a]* Charles L. Barnes[b] and Thomas P. Mawhinney[a]

[a]Department of Biochemistry, University of Missouri, Columbia, MO 65211, USA, and [b]Department of Chemistry, University of Missouri, Columbia, MO 65211, USA. *Correspondence e-mail: mossinev@missouri.edu

Received 29 December 2017
Accepted 2 January 2018

Edited by P. McArdle, National University of Ireland, Ireland

Keywords: crystal structure; D-fructosamine; acyclic carbohydrate; Hirshfeld surface analysis.

CCDC reference: 1811885

Supporting information: this article has supporting information at journals.iucr.org/e

The title compound, $C_{14}H_{21}NO_6$, (I), crystallizes exclusively in the acyclic *keto* form. In solution of (I), the acyclic tautomer represents only 10% of the population in equilibrium, with the other 90% consisting of β-pyranose, β-furanose, α-pyranose, and α-furanose cyclic forms. The carbohydrate chain in (I) has a zigzag conformation and the aromatic amine group has a transitional sp^2/sp^3 geometry. Bond lengths and valence angles in the carbohydrate portion compare well with the average values for related acyclic polyol structures. All of the hydroxyl groups are involved in intermolecular hydrogen bonding and form a two-dimensional network of infinite chains, which are interlinked by intramolecular hydrogen bonds and organized into $R_8^8(16)$ homodromic ring patterns. A comparative Hirshfeld surfaces analysis of (I) and four other 1-amino-1-deoxy-D-fructose derivatives suggests the balance of hydrophilic/hydrophobic interactions plays a role in the crystal packing, favoring the acyclic isomer.

1. Chemical context

Reducing carbohydrates, for instance aldoses (glucose, mannose, xylose) or ketoses (fructose, ribulose), mutarotate in solutions such that the predominant species in equilibrium consist of cyclic pyranose and furanose hemiacetals or hemiketals, respectively (Angyal, 1992). Free aldehyde or ketone forms are thermodynamically unfavorable and normally comprise less than 1% of the population in the equilibria. Crystallization of reducing monosaccharides naturally affords the most populous, predominantly pyranose, anomers (Jeffrey, 1990). Previously, we have demonstrated that exceptions to this rule may be found among 1-amino-1-deoxy-ketoses. Only four acyclic ketosamine structures have been accurately characterized by X-ray diffraction so far (Mossine *et al.*, 1995, 2002, 2009); however, it was suggested that the hydrophobic nature of the amino substituents may play a supporting role in stabilization of the unique structures (Mossine *et al.*, 2009). Given that the concept of acyclic intermediates is essential for understanding the mechanisms of many enzymatic and non-enzymatic transformations of carbohydrates in general (see, for example, Buchholz & Seibel, 2008; Wang *et al.*, 2014) and natural fructosamines in particular (Nursten, 2005), the availability of precise structural knowledge on the open-chain 1-amino-1-deoxy-ketoses is of interest to the field. We report here on the structure of title compound, alternatively named as D-fructose-*N*-methyl-*p*-anisidine, $C_{14}H_{21}NO_6$, (I), aiming to expand this knowledge.

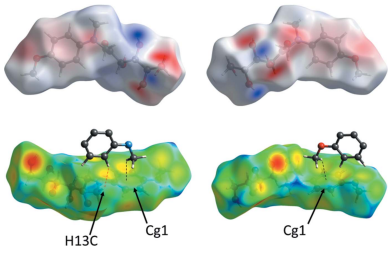

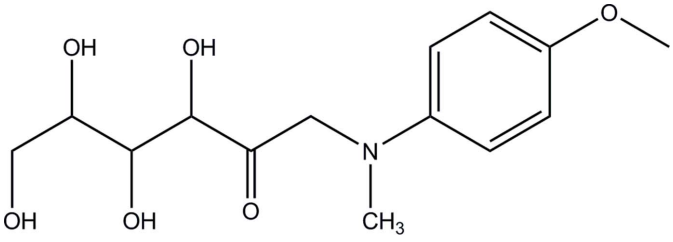

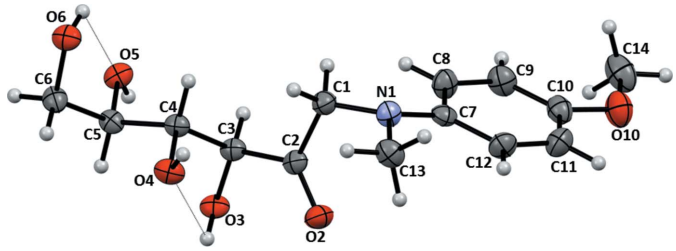

Figure 1
Atomic numbering and displacement ellipsoids at the 50% probability level for (I). Intramolecular O—H···O interactions are shown as dotted lines.

2. Structural commentary

The molecular structure and atomic numbering for (I) are shown in Fig. 1. The molecule may be considered as a conjugate of a carbohydrate, 1-amino-1-deoxy-D-fructose, and an aromatic amine, *N*-methyl-*p*-anisidine, which are joined through the common amino group. The carbohydrate portion in (I) exists in the acyclic *keto* form. Remarkably, in the aqueous solution of (I), the acyclic *keto* form is a minor constituent of the established equilibrium, at 10.3% of the total population as follows from the ^{13}C NMR data (Table 1). The predominant β-pyranose anomer (52.0%) and smaller proportions of the β-furanose, α-pyranose, and α-furanose cyclic forms constitute the rest of the equilibrium composition (Fig. 2).

The carbohydrate fragment of the molecule is in the *zigzag* conformation, having four out of six of its carbon atoms, C3, C4, C5, and C6, located in one plane. The conformation around the carbonyl group is also nearly flat and involves atoms N1, C1, C2, O2, C3, and O3, with the carbonyl O2 in the *syn-periplanar* position with respect to both N1 and O3 [respective torsion angles are 11.7 (3) and −7.0 (3)°]. This type of conformation is preferred for the β-aminocarbonyl group, due to influence of the $\sigma_{C-H} \rightarrow \sigma_{C=O}^*$ and $\sigma_{C-H} \rightarrow \pi_{C=O}^*$ hyperconjugation in conditions when interaction between the nitrogen lone pair (LP) and the carbonyl π^*-system is not significant (Ducati *et al.*, 2006). Indeed, the LP—N1—C1—C2 torsion angle estimate is close to 180° in (I). In the sugar portion of (I), the average C—O bond distances (1.43 ± 0.01Å) and the valence angles in hydroxyl groups are close to the average values for a number of crystalline alditol structures (Jeffrey & Kim, 1970) and acyclic ketosamines (Mossine *et al.*, 1995, 2002, 2009). Two heteroatom contacts, O3—H···O4 and O6—H···O5, although weakly directional

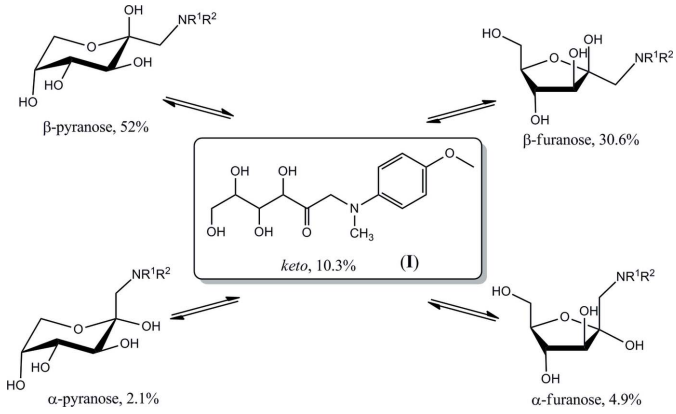

Figure 2
Isomerization equilibrium of (I) in solution.

(Table 2), are cooperatively integrated into the hydrogen-bonding scheme (see Section 3) and thus are good candidates to qualify for intramolecular hydrogen bonds. The tertiary amino group geometry is a flattened pyramid, with the distance from the N1 apex to the C1–C7–C13 base being 0.219 Å and the average base-face dihedral angle 17.2°. The N1—C7 distance, at 1.403 Å, is significantly shorter than the distances from N1 to the aliphatic carbons C1 and C13 [1.444 (3) and 1.455 (3) Å]. Such geometry is characteristic for amino groups with a mixed sp^3/sp^2 hybridization, likely due to a partial resonance of the nitrogen *p*-electrons with a neighboring π-system, such as the benzene ring in (I). In the solid-state ^{13}C NMR spectrum (Fig. 3), the peaks corresponding to the carbons C1, C7, and C13 are split, indicating a conformational dimorphism of the tertiary amino group, possibly due to an inversion of configuration at the N1 atom.

Table 1
Distribution (%) of cyclic and acyclic forms of some 1-amino-1-deoxy-D-fructose derivatives in D_2O/pyridine (1:1) at 293 K, as estimated from the ^{13}C NMR spectra, and in the crystalline state.

Compound	α-pyranose	β-pyranose	α-furanose	β-furanose	acyclic, *keto*	Crystalline isomers
(I)	2.1	52.0	4.9	30.6	10.3	acyclic *keto*
FruNMpti[a]	2.1	49.9	4.8	32.2	11.0	acyclic *keto*
FruNEpca[a]	2.0	48.7	4.2	32.3	12.7	acyclic *keto*
Frupti[a,b]	3.5	61.0	9.4	24.2	1.9	β-pyranose
FruAlla[c]	2.2	47.4	4.5	33.6	12.3	β-pyranose
Fructosamine[d]	5.0	70.8	11.2	12.3	0.8	β-pyranose
FruAib[e]	3.0	75.6	10.1	10.4	<0.7	β-pyranose

Notes: (*a*) Mossine *et al.* (2009); (*b*) Gomez de Anderez *et al.* (1996); (*c*) Mossine *et al.* (2009*a*); (*d*) Mossine *et al.* (2009*b*); (*e*) Mossine *et al.* (2018).

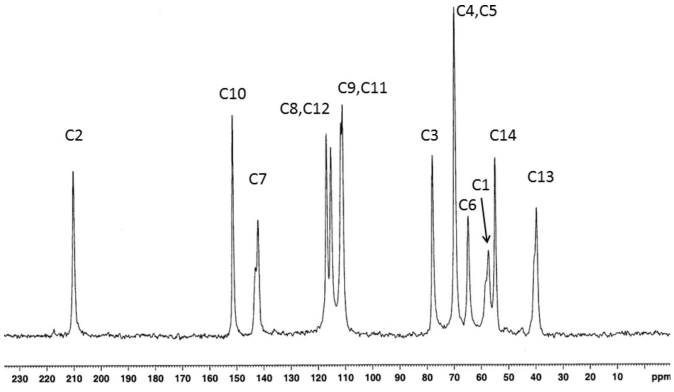

Figure 3
Solid-state ^{13}C NMR spectrum of powdered crystalline (I).

3. Supramolecular features

Compound (I) crystallizes in the monoclinic space group $P2_1$, with two equivalent molecules per unit cell. The molecular packing of (I) features 'hydrophilic' and 'hydrophobic' layers propagating in the *ab* plane (Fig. 4). The carbohydrate residues form a two-dimensional network of hydrogen bonds organized as a system of two homodromic infinite chains, with ···O3—H···O5—H··· and ···O4—H···O6—H··· recurrent sequences of intermolecular hydrogen bonds. These chains are topologically connected by the intramolecular short heteroatom contacts O3—H···O4 and O6—H···O5. Basic hydrogen-bonding patterns of the resulting network are depicted in Fig. 5 and include fused homodromic $R_8^8(16)$ and antidromic $R_2^2(4)$ rings (the pattern notation according to Bernstein *et al.*, 1995). The intermolecular heteroatom contacts that define the hydrogen bonding in (I) are not confined exclusively to the carbohydrate portion of the molecule (Fig. 6), however. In addition, there are two close C—H···O2 contacts involving the carbonyl group, and two short C—H···π contacts between the methyl groups and the benzene ring centroids (*Cg*1), which may qualify as weak hydrogen bonds (Table 3, Fig. 6). The Hirshfeld surface analysis (Spackman & Jayatilaka, 2009) revealed that a major proportion of the intermolecular contacts in crystal structure of (I) is provided by non- or low-polar interactions of the H···H and C···H type (Fig. 7 and Table 4).

Table 2
Hydrogen-bond geometry (Å, °).

D—H···*A*	*D*—H	H···*A*	*D*···*A*	*D*—H···*A*
O3—H3*O*···O4	0.87 (3)	2.67 (3)	2.962 (2)	101 (3)
O3—H3*O*···O5^{i}	0.87 (3)	1.94 (3)	2.747 (2)	153 (2)
O4—H4*O*···O6^{ii}	0.80 (3)	1.90 (3)	2.700 (2)	176 (3)
O5—H5*O*···O3^{iii}	0.86 (3)	1.86 (3)	2.702 (2)	165 (3)
O6—H6*O*···O5	0.82 (3)	2.56 (3)	2.918 (2)	108 (3)
O6—H6*O*···O4^{iv}	0.82 (3)	1.95 (3)	2.704 (2)	154 (3)

Symmetry codes: (i) $x, y+1, z$; (ii) $-x, y+\frac{1}{2}, -z+2$; (iii) $-x+1, y-\frac{1}{2}, -z+2$; (iv) $x, y-1, z$.

Table 3
Suspected C—H···*A* contacts (Å, °).

C—H···*A*	C—H	H···*A*	C···*A*	C—H···*A*	Symmetry
C1—H1*A*···O2	0.99	2.48	3.386 (3)	152	$x, y-1, z$
C14—H14*B*···O2	0.98	2.52	3.311 (3)	138	$-x+1, y-\frac{1}{2}, -z+1$
C14—H14*A*···*Cg*1	0.98	2.95	3.747 (3)	139	$-x+1, y-\frac{1}{2}, -z+1$
C13—H13*C*···*Cg*1	0.98	2.80	3.539 (2)	133	$-x, y+\frac{1}{2}, -z+1$

4. Database survey

A search of SciFinder, Google Scholar, and the Cambridge Structural Database (Groom *et al.*, 2016) by both structure and chemical names for 1-deoxy-1-(*N*-methyl-*p*-methoxyphenylamino)-D-fructose returned no references; hence compound (I) is new. There are four closely related structures, namely D-fructose-*N*-methyl-*p*-toluidine (FruNMpti, CCDC 717802),

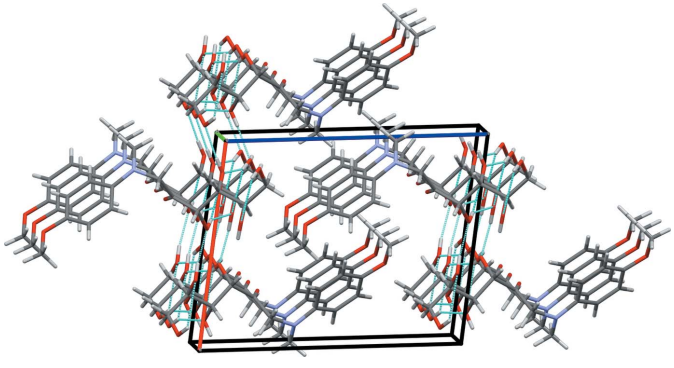

Figure 4
The molecular packing in (I). Color code for crystallographic axes: red – *a*, green – *b*, blue – *c*. Hydrogen bonds are shown as cyan dotted lines.

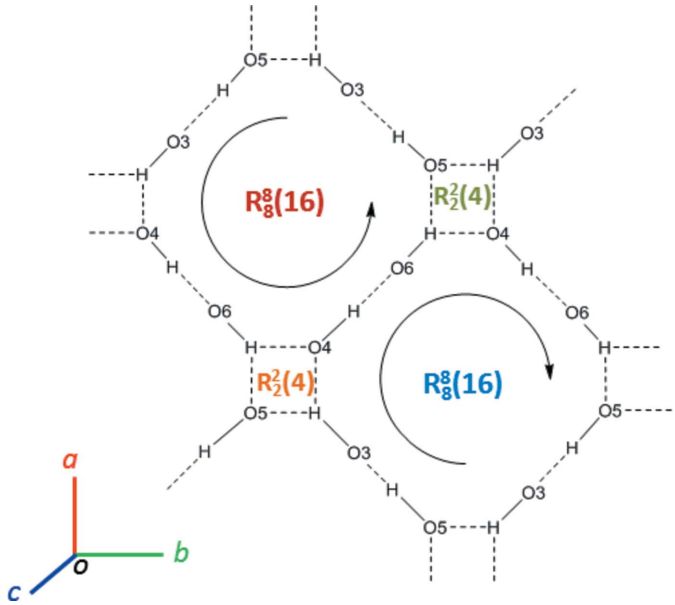

Figure 5
Hydrogen-bonding pattern in the crystal structure of (I).

Table 4
Contributions (%) of specific contact types to the Hirshfeld surfaces of 1-amino-1-deoxy-D-fructose derivatives.

Compound	Conformation	O···H	H···H	C···H	Other contacts
(I)	acyclic *keto*	32.3	52.8	13.2	N···H 1.6; C···C 0.1
FruNMpti[a]	acyclic *keto*	26.5	59.8	11.8	N···H 1.6; C···C 0.3
FruNEpca[a]	acyclic *keto*	23.1	50.1	8.6	N···C 0.5; C···C 1.3; Cl···H 13.1; Cl···C 3.4
FruNAlla[b]	β-pyranose	15.2	67.7	16.9	C···C 0.1
FruNBn$_2$[c]	β-pyranose	16.5	64.2	19.2	C···O 0.1
TagNMBn[d]	α-pyranose	20.6	65.8	13.5	O···O 0.1

Notes: (*a*) Mossine *et al.* (2009); (*b*) Mossine *et al.* (2009*a*); (*c*) Hou *et al.* (2001); (*d*) Pérez *et al.* (1978).

D-fructose-*p*-toluidine (Frupti, CCDC 126260), D-fructose-*N*-ethyl-*p*-chloroaniline (FruNEpca, CCDC 717803), and D-fructose-*N*-allylaniline (FruNAlla, CCDC 717417). Each of these 1-amino-1-deoxy-D-fructose derivatives features an aromatic substituent at the amino group. They also display a similar to (I) distribution of the cyclic and acyclic tautomeric forms in solutions (Table 1). However, only FruNMpti and FruNEpca were reported to adopt the acyclic *keto* conformations in crystalline state. Frupti (Gomez de Anderez *et al.*, 1996), FruNAlla (Mossine *et al.*, 2009*a*), as well as the rest of the 1-amino-1-deoxy-D-fructose derivatives whose structures were solved by X-ray diffraction methods (about 15 structures so far), crystallize in the β-D-fructopyranose anomeric form (Table 1). The unusual propensity of some 1-amino-1-deoxy-D-fructose derivatives, including (I), to crystallize in a thermodynamically unfavored acyclic form is difficult to explain, given that the number of the available solved structures is thus far too small. Modelling the energies of intermolecular interactions experienced by these molecules in solutions *versus* crystal environments was beyond the goals of the current study. However, some initial clues can be derived from analysis of data compiled in Table 1, this work, as well as in Table 1 from our previous study (Mossine *et al.*, 2009). First, only fructosamine derivatives decorated with an aromatic amino substituent can, but not always, crystallize as the acyclic *keto* tautomer. As pointed out in Section 2, a neighboring π-system may resonate with the amine *p*-electrons thus making them unavailable for σ-bonding. Next, among *N*-aryl derivatives of 1-amino-1-deoxy-D-fructose, only those lacking a proton bound to the tertiary amino group can crystallize in the acyclic form. Indeed, no hydrogen bonds involving N1 were detected in acyclic (I), FruNMpti or FruNEpca (Mossine *et al.*, 2009). In contrast, the structures of Frupti, FruAlla and all the rest of the 1-amino-1-deoxy-D-fructose derivatives reveal at least one hydrogen-mediated intramolecular heteroatom contact between the amino nitrogen atom and an oxygen atom originating from the carbohydrate portion of the molecule, most often the anomeric O2. Thus, the inability of the amino group to form stable intramolecular hydrogen bonds with the carbohydrate portion plays a role in stabilization of the acyclic tautomer. Finally, a comparative Hirshfeld surfaces analysis (Table 4) of these structures suggests that the extended linear conformation of the acyclic tautomer may require more of the 'hydrophilic space' available in the crystal structure, as compared to the pyranose anomers. This argument also seems

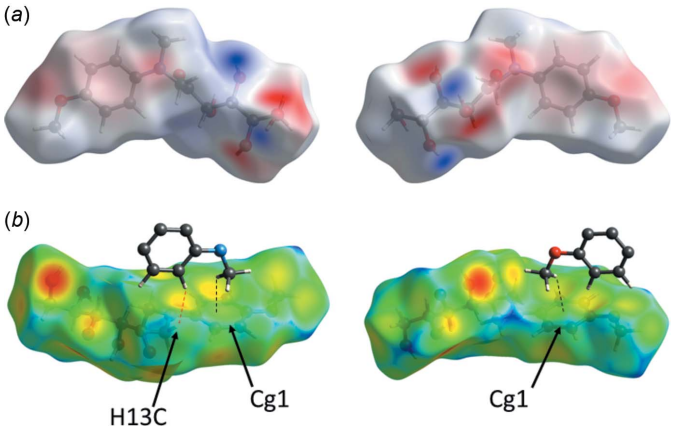

Figure 6
Views of the Hirshfeld surface for (I) mapped over: (*a*) the electrostatic potential in the range −0.0966 to +0.1843 a.u. The red and blue colors represent the distribution of the negative and positive electrostatic potential, respectively; (*b*) the d_e function, in the range 0.683 to 2.484 Å, calculated for the external contact atoms in the crystal. Shown are molecular fragments involved in the C—H···π interactions (black dotted lines) and the shortest H···H contact (red dotted line).

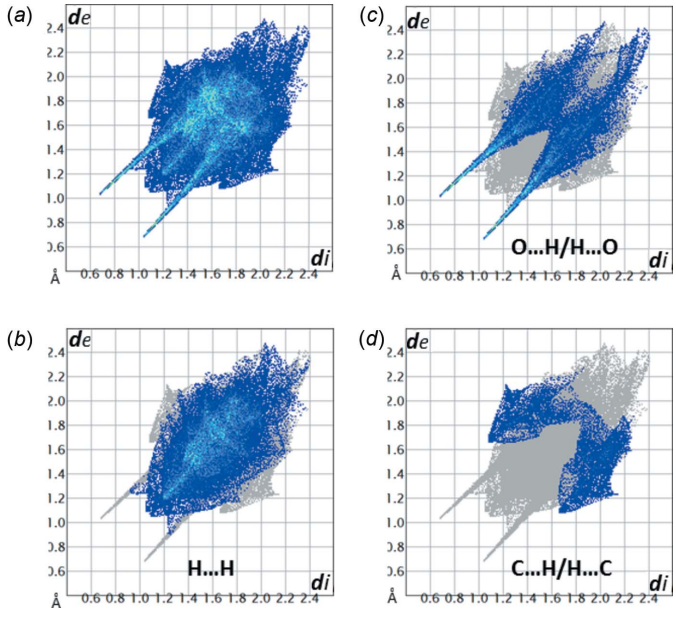

Figure 7
(*a*) The full two-dimensional fingerprint plot for (I) and those delineated for the specific contacts: (*b*) O···H; (*c*) H···H; (*d*) C···H.

Table 5
Experimental details.

Crystal data	
Chemical formula	$C_{14}H_{21}NO_6$
M_r	299.32
Crystal system, space group	Monoclinic, $P2_1$
Temperature (K)	100
a, b, c (Å)	10.8002 (15), 5.1439 (7), 13.3931 (19)
β (°)	98.382 (1)
V (Å^3)	736.11 (18)
Z	2
Radiation type	Mo $K\alpha$
μ (mm^{-1})	0.11
Crystal size (mm)	0.35 × 0.15 × 0.12
Data collection	
Diffractometer	Bruker APEXII CCD area detector
Absorption correction	Multi-scan (*SADABS*; Sheldrick (2003)
T_{min}, T_{max}	0.88, 0.99
No. of measured, independent and observed [$I > 2\sigma(I)$] reflections	8031, 2993, 2788
R_{int}	0.026
(sin $\theta/\lambda)_{max}$ (Å^{-1})	0.625
Refinement	
$R[F^2 > 2\sigma(F^2)]$, $wR(F^2)$, S	0.031, 0.082, 1.04
No. of reflections	2993
No. of parameters	208
No. of restraints	1
H-atom treatment	H atoms treated by a mixture of independent and constrained refinement
$\Delta\rho_{max}$, $\Delta\rho_{min}$ (e Å^{-3})	0.19, −0.15
Absolute structure	Flack x determined using 1149 quotients $[(I^+)-(I^-)]/[(I^+)+(I^-)]$ (Parsons *et al.*, 2013)
Absolute structure parameter	0.3 (5)

Computer programs: *SMART* and *SAINT* (Bruker, 1998), *SHELXS97* (Sheldrick, 2008), *SHELXL2017/1* (Sheldrick, 2015), *X-SEED* (Barbour, 2001), *Mercury* (Macrae *et al.*, 2008), *CIFTAB* (Sheldrick, 2008) and *publCIF* (Westrip, 2010).

to be supported by an observation that an increase in size of the *N*-substituents, such as from methyl or ethyl (in FruNMpti and FruNEpca) to allyl or butyl (in FruAlla and D-fructose-*N*-butylaniline), leads to a loss of propensity to crystallize in the acyclic form (Mossine *et al.*, 2009).

5. Synthesis and crystallization

The preparation of (I) was performed following a protocol described previously (Mossine *et al.*, 2009). Briefly, a mixture of 5.4 g (0.03 moles) of D-glucose, 2.7 g (0.022 moles) of *p*-anisidine and 0.55 mL of 3-mercaptopropionic acid catalyst/antioxidant was stirred for 6 h in 12 mL of isopropanol in a screw-capped glass vial at 360 K. The reaction progress was followed by TLC. The purification step included an ion-exchange on Amberlite IRN-77 (H^+), with 0.2 *M* NH_4OH in 50% ethanol as an eluant, and was followed by flash filtration on a short silica column using 5% MeOH in CH_2Cl_2 as an eluant. Crystallization of the compound was aided by the addition of a small amount of acetone to the syrupy evaporation residue. The crystals were filtered off, washed with acetone and dried *in vacuo* over $CaCl_2$, yield 1.6 g (27%, based on starting amine) of colorless prisms. Major (β-pyranose anomer) peaks (ppm) in the ^{13}C NMR spectrum in D_2O/pyridine: 154.14 (C10); 148.12 (C7); 117.86, 117.11 (C8, C12); 116.96, 116.80 (C9, C11); 101.56 (C2); 72.98 (C4); 71.99 (C3, C5); 65.90 (C6); 63.21 (C1); 57.84 (C14); 42.62 (C13). The ^{13}C CPMAS–TOSS spectrum of finely powdered crystalline (I) is shown in Fig. 3 and the minor peak assignments are listed in Supplementary Table S1.

6. Refinement

Crystal data, data collection and structure refinement details are summarized in Table 5. Hydroxy and nitrogen-bound H atoms were located in difference-Fourier analyses and were allowed to refine fully. Other H atoms were placed at calculated positions and treated as riding, with C—H = 0.98 Å (methyl), 0.99 Å (methylene) or 1.00 Å (methine) and with U_{iso}(H) = 1.2U_{eq}(methine or methylene) or 1.5U_{eq}(methyl). The Flack absolute structure parameter determined [0.3 (5) for 1149 quotients (Parsons *et al.*, 2013)] is consistent with the (3*S*,4*R*,5*R*) configuration which was assigned for this chain system on the basis of the known configuration for the starting material D-glucose (McNaught, 1996).

Funding information

Funding for this research was provided by: University of Missouri Agriculture Experiment Station Chemical Laboratories.

References

Angyal, S. J. (1992). *Adv. Carbohydr. Chem. Biochem.* **49**, 19–35.
Barbour, L. J. (2001). *J. Supramol. Chem.* **1**, 189–191.
Bernstein, J., Davis, R. E., Shimoni, L. & Chang, N.-L. (1995). *Angew. Chem. Int. Ed. Engl.* **34**, 1555–1573.
Bruker. (1998). *SMART* and *SAINT-Plus*. Bruker AXS Inc., Madison, Wisconsin, USA.
Buchholz, K. & Seibel, J. (2008). *Carbohydr. Res.* **343**, 1966–1979.
Ducati, L. C., Rittner, R. & Custódio, R. (2006). *J. Mol. Struct. Theochem*, **766**, 177–183.
Gomez de Anderez, D., Gil, H., Helliwell, M. & Mata Segreda, J. (1996). *Acta Cryst.* C**52**, 252–254.
Groom, C. R., Bruno, I. J., Lightfoot, M. P. & Ward, S. C. (2016). *Acta Cryst.* B**72**, 171–179.
Hou, Y., Wu, X., Xie, W., Braunschweiger, P. G. & Wang, P. G. (2001). *Tetrahedron Lett.* **42**, 825–829.
Jeffrey, G. A. (1990). *Acta Cryst.* B**46**, 89–103.
Jeffrey, G. A. & Kim, H. S. (1970). *Carbohydr. Res.* **14**, 207–216.
Macrae, C. F., Bruno, I. J., Chisholm, J. A., Edgington, P. R., McCabe, P., Pidcock, E., Rodriguez-Monge, L., Taylor, R., van de Streek, J. & Wood, P. A. (2008). *J. Appl. Cryst.* **41**, 466–470.
McNaught, A. D. (1996). *Pure Appl. Chem.* **68**, 1919–2008.
Mossine, V. V., Barnes, C. L., Chance, D. L. & Mawhinney, T. P. (2009). *Angew. Chem. Int. Ed.* **48**, 5517–5520.
Mossine, V. V., Barnes, C. L., Feather, M. S. & Mawhinney, T. P. (2002). *J. Am. Chem. Soc.* **124**, 15178–15179.
Mossine, V. V., Barnes, C. L., Glinsky, G. V. & Feather, M. S. (1995). *Carbohydr. Lett.* **1**, 355–362.
Mossine, V. V., Barnes, C. L. & Mawhinney, T. P. (2009*a*). *Carbohydr. Res.* **344**, 948–951.

Mossine, V. V., Barnes, C. L. & Mawhinney, T. P. (2009*b*). *J. Carbohydr. Chem.* **28**, 245–263.
Mossine, V. V., Barnes, C. L. & Mawhinney, T. P. (2018). *Acta Cryst*. E**74**, 72–77.
Nursten, H. (2005). *The Maillard Reaction: Chemistry, Biochemistry and Implications*. Cambridge: The Royal Society of Chemistry.
Parsons, S., Flack, H. D. & Wagner, T. (2013). *Acta Cryst.* B**69**, 249–259.
Pérez, S., López-Castro, A. & Márquez, R. (1978). *Acta Cryst.* B**34**, 2341–2344.
Sheldrick, G. M. (2003). *SADABS*. University of Göttingen, Germany.
Sheldrick, G. M. (2008). *Acta Cryst.* A**64**, 112–122.
Sheldrick, G. M. (2015). *Acta Cryst.* C**71**, 3–8.
Spackman, M. A. & Jayatilaka, D. (2009). *CrystEngComm*, **11**, 19–32.
Wang, T., Nolte, M. W. & Shanks, B. H. (2014). *Green Chem.* **16**, 548–572.
Westrip, S. P. (2010). *J. Appl. Cryst.* **43**, 920–925.

supporting information

Acta Cryst. (2018). E**74**, 127-132 [https://doi.org/10.1107/S2056989018000099]

Crystal structure of the acyclic form of 1-deoxy-1-[(4-methoxyphenyl)(methyl)-amino]-D-fructose

Valeri V. Mossine, Charles L. Barnes and Thomas P. Mawhinney

Computing details

Data collection: *SMART* (Bruker, 1998); cell refinement: *SAINT* (Bruker, 1998); data reduction: *SAINT* (Bruker, 1998); program(s) used to solve structure: *SHELXS97* (Sheldrick, 2008); program(s) used to refine structure: *SHELXL2017/1* (Sheldrick, 2015); molecular graphics: *X-SEED* (Barbour, 2001) and *Mercury* (Macrae *et al.*, 2008); software used to prepare material for publication: *CIFTAB* (Sheldrick, 2008) and *publCIF* (Westrip, 2010).

1-Deoxy-1-[(4-methoxyphenyl)(methyl)amino]-*D*-fructose

Crystal data

$C_{14}H_{21}NO_6$
M_r = 299.32
Monoclinic, $P2_1$
a = 10.8002 (15) Å
b = 5.1439 (7) Å
c = 13.3931 (19) Å
β = 98.382 (1)°
V = 736.11 (18) Å^3
Z = 2
$F(000)$ = 320
D_x = 1.350 Mg m^{-3}
Mo $K\alpha$ radiation, λ = 0.71073 Å
Cell parameters from 3774 reflections
θ = 2.6–25.8°
μ = 0.11 mm^{-1}
T = 100 K
Prism, colourless
0.35 × 0.15 × 0.12 mm

Data collection

Bruker APEXII CCD area detector diffractometer
ω scans
Absorption correction: multi-scan (SADABS; Sheldrick (2003)
T_{min} = 0.88, T_{max} = 0.99
8031 measured reflections
2993 independent reflections
2788 reflections with $I > 2\sigma(I)$
R_{int} = 0.026
θ_{max} = 26.4°, θ_{min} = 1.9°
h = −13→13
k = −6→6
l = −16→16

Refinement

Refinement on F^2
Least-squares matrix: full
$R[F^2 > 2\sigma(F^2)]$ = 0.031
$wR(F^2)$ = 0.082
S = 1.04
2993 reflections
208 parameters
1 restraint
Hydrogen site location: mixed
H atoms treated by a mixture of independent and constrained refinement
$w = 1/[\sigma^2(F_o^2) + (0.0443P)^2 + 0.0803P]$ where $P = (F_o^2 + 2F_c^2)/3$
$(\Delta/\sigma)_{max} < 0.001$
$\Delta\rho_{max}$ = 0.19 e Å^{-3}
$\Delta\rho_{min}$ = −0.15 e Å^{-3}
Absolute structure: Flack x determined using 1149 quotients $[(I^+)-(I^-)]/[(I^+)+(I^-)]$ (Parsons *et al.*, 2013)
Absolute structure parameter: 0.3 (5)

Special details

Geometry. All esds (except the esd in the dihedral angle between two l.s. planes) are estimated using the full covariance matrix. The cell esds are taken into account individually in the estimation of esds in distances, angles and torsion angles; correlations between esds in cell parameters are only used when they are defined by crystal symmetry. An approximate (isotropic) treatment of cell esds is used for estimating esds involving l.s. planes.

Fractional atomic coordinates and isotropic or equivalent isotropic displacement parameters (Å²)

	x	*y*	*z*	U_{iso}*/U_{eq}
N1	0.10655 (16)	0.5973 (4)	0.64477 (12)	0.0275 (4)
C1	0.15040 (19)	0.4862 (4)	0.74257 (15)	0.0267 (4)
H1A	0.189953	0.316322	0.732685	0.032*
H1B	0.077318	0.453299	0.777617	0.032*
O2	0.26415 (14)	0.8787 (3)	0.79127 (12)	0.0321 (4)
C2	0.24391 (18)	0.6543 (4)	0.81040 (15)	0.0240 (4)
O3	0.40317 (13)	0.6914 (3)	0.95778 (11)	0.0268 (3)
C3	0.31015 (18)	0.5253 (4)	0.90646 (15)	0.0229 (4)
H3	0.352434	0.364549	0.886440	0.027*
O4	0.13795 (14)	0.6653 (3)	0.99012 (12)	0.0281 (3)
C4	0.21360 (18)	0.4440 (4)	0.97432 (14)	0.0220 (4)
H4	0.159267	0.302656	0.940569	0.026*
O5	0.35348 (13)	0.1285 (3)	1.06292 (11)	0.0270 (3)
C5	0.27762 (17)	0.3493 (4)	1.07730 (15)	0.0231 (4)
H5	0.332604	0.491086	1.109907	0.028*
O6	0.09673 (13)	0.0803 (3)	1.10474 (11)	0.0285 (3)
C6	0.18494 (19)	0.2727 (5)	1.14715 (15)	0.0285 (5)
H6A	0.231641	0.204885	1.210924	0.034*
H6B	0.138815	0.429609	1.163615	0.034*
C7	0.18576 (18)	0.5977 (4)	0.57050 (15)	0.0250 (4)
C8	0.2825 (2)	0.4181 (5)	0.57062 (16)	0.0322 (5)
H8	0.300894	0.301939	0.625936	0.039*
C9	0.3529 (2)	0.4053 (5)	0.49151 (17)	0.0352 (5)
H9	0.417860	0.280262	0.493123	0.042*
O10	0.39239 (16)	0.5762 (4)	0.32846 (12)	0.0437 (4)
C10	0.3286 (2)	0.5736 (5)	0.41076 (16)	0.0319 (5)
C11	0.2348 (2)	0.7560 (5)	0.41043 (17)	0.0352 (5)
H11	0.218288	0.874400	0.355652	0.042*
C12	0.1644 (2)	0.7690 (5)	0.48871 (16)	0.0316 (5)
H12	0.100474	0.896471	0.486890	0.038*
C13	0.0158 (2)	0.8065 (5)	0.64424 (17)	0.0330 (5)
H13A	0.059076	0.974339	0.646201	0.050*
H13B	−0.027328	0.790523	0.703438	0.050*
H13C	−0.045390	0.795655	0.582714	0.050*
C14	0.4858 (2)	0.3812 (7)	0.3254 (2)	0.0474 (7)
H14A	0.551236	0.401318	0.383834	0.071*
H14B	0.522812	0.399739	0.263176	0.071*
H14C	0.447653	0.208769	0.327161	0.071*
H5O	0.430 (3)	0.175 (7)	1.061 (2)	0.050 (8)*

H4O	0.069 (3)	0.643 (7)	0.959 (2)	0.052 (9)*
H6O	0.133 (3)	−0.034 (6)	1.078 (2)	0.047 (8)*
H3O	0.368 (2)	0.835 (6)	0.974 (2)	0.041 (8)*

Atomic displacement parameters (Å²)

	U^{11}	U^{22}	U^{33}	U^{12}	U^{13}	U^{23}
N1	0.0270 (9)	0.0286 (9)	0.0267 (9)	0.0036 (8)	0.0032 (7)	0.0003 (7)
C1	0.0277 (11)	0.0254 (10)	0.0268 (10)	−0.0020 (9)	0.0032 (8)	0.0011 (8)
O2	0.0344 (8)	0.0240 (8)	0.0372 (9)	−0.0023 (7)	0.0026 (7)	0.0027 (7)
C2	0.0207 (9)	0.0242 (10)	0.0288 (10)	0.0003 (8)	0.0099 (8)	−0.0007 (8)
O3	0.0166 (7)	0.0272 (8)	0.0365 (8)	−0.0027 (6)	0.0038 (6)	−0.0025 (6)
C3	0.0180 (9)	0.0223 (10)	0.0287 (10)	−0.0003 (7)	0.0048 (8)	−0.0013 (8)
O4	0.0178 (7)	0.0281 (8)	0.0383 (8)	0.0029 (6)	0.0040 (6)	−0.0057 (6)
C4	0.0172 (9)	0.0220 (10)	0.0274 (10)	0.0011 (7)	0.0052 (8)	−0.0023 (8)
O5	0.0168 (7)	0.0276 (8)	0.0368 (8)	0.0007 (6)	0.0045 (6)	0.0031 (6)
C5	0.0164 (9)	0.0270 (10)	0.0261 (10)	−0.0009 (8)	0.0037 (8)	−0.0033 (8)
O6	0.0190 (7)	0.0306 (8)	0.0370 (8)	−0.0016 (6)	0.0081 (6)	−0.0033 (7)
C6	0.0229 (10)	0.0363 (12)	0.0266 (10)	−0.0059 (9)	0.0043 (8)	−0.0020 (10)
C7	0.0244 (9)	0.0235 (10)	0.0258 (10)	−0.0023 (8)	−0.0012 (8)	−0.0044 (8)
C8	0.0327 (11)	0.0344 (12)	0.0288 (11)	0.0070 (10)	0.0021 (9)	0.0038 (9)
C9	0.0313 (11)	0.0390 (14)	0.0353 (12)	0.0084 (10)	0.0054 (9)	−0.0012 (10)
O10	0.0399 (9)	0.0585 (11)	0.0354 (9)	0.0012 (9)	0.0143 (7)	−0.0009 (8)
C10	0.0281 (11)	0.0398 (13)	0.0283 (10)	−0.0043 (10)	0.0055 (8)	−0.0046 (10)
C11	0.0376 (13)	0.0344 (12)	0.0335 (12)	0.0000 (10)	0.0054 (10)	0.0080 (10)
C12	0.0326 (11)	0.0263 (11)	0.0355 (12)	0.0058 (9)	0.0033 (9)	0.0040 (10)
C13	0.0294 (11)	0.0350 (13)	0.0346 (11)	0.0058 (10)	0.0044 (9)	−0.0031 (10)
C14	0.0331 (12)	0.0692 (19)	0.0416 (14)	0.0003 (13)	0.0115 (10)	−0.0126 (13)

Geometric parameters (Å, º)

N1—C7	1.403 (3)	O6—H6O	0.82 (3)
N1—C1	1.444 (3)	C6—H6A	0.9900
N1—C13	1.455 (3)	C6—H6B	0.9900
C1—C2	1.525 (3)	C7—C8	1.395 (3)
C1—H1A	0.9900	C7—C12	1.399 (3)
C1—H1B	0.9900	C8—C9	1.392 (3)
O2—C2	1.209 (3)	C8—H8	0.9500
C2—C3	1.529 (3)	C9—C10	1.380 (3)
O3—C3	1.418 (2)	C9—H9	0.9500
O3—H3O	0.87 (3)	O10—C10	1.382 (3)
C3—C4	1.538 (3)	O10—C14	1.428 (3)
C3—H3	1.0000	C10—C11	1.381 (3)
O4—C4	1.435 (2)	C11—C12	1.383 (3)
O4—H4O	0.80 (3)	C11—H11	0.9500
C4—C5	1.530 (3)	C12—H12	0.9500
C4—H4	1.0000	C13—H13A	0.9800
O5—C5	1.430 (2)	C13—H13B	0.9800

O5—H5O	0.86 (3)	C13—H13C	0.9800
C5—C6	1.518 (3)	C14—H14A	0.9800
C5—H5	1.0000	C14—H14B	0.9800
O6—C6	1.432 (3)	C14—H14C	0.9800

C7—N1—C1	119.35 (16)	C5—C6—H6A	108.9
C7—N1—C13	118.38 (17)	O6—C6—H6B	108.9
C1—N1—C13	115.40 (17)	C5—C6—H6B	108.9
N1—C1—C2	114.64 (18)	H6A—C6—H6B	107.7
N1—C1—H1A	108.6	C8—C7—C12	117.14 (18)
C2—C1—H1A	108.6	C8—C7—N1	122.18 (19)
N1—C1—H1B	108.6	C12—C7—N1	120.53 (19)
C2—C1—H1B	108.6	C9—C8—C7	121.5 (2)
H1A—C1—H1B	107.6	C9—C8—H8	119.3
O2—C2—C1	122.7 (2)	C7—C8—H8	119.3
O2—C2—C3	121.04 (19)	C10—C9—C8	120.3 (2)
C1—C2—C3	116.29 (17)	C10—C9—H9	119.9
C3—O3—H3O	109.2 (18)	C8—C9—H9	119.9
O3—C3—C2	110.97 (16)	C10—O10—C14	116.9 (2)
O3—C3—C4	111.77 (16)	C9—C10—C11	118.96 (19)
C2—C3—C4	109.93 (15)	C9—C10—O10	124.8 (2)
O3—C3—H3	108.0	C11—C10—O10	116.2 (2)
C2—C3—H3	108.0	C10—C11—C12	121.0 (2)
C4—C3—H3	108.0	C10—C11—H11	119.5
C4—O4—H4O	108 (2)	C12—C11—H11	119.5
O4—C4—C5	108.19 (15)	C11—C12—C7	121.1 (2)
O4—C4—C3	108.74 (16)	C11—C12—H12	119.4
C5—C4—C3	111.30 (15)	C7—C12—H12	119.4
O4—C4—H4	109.5	N1—C13—H13A	109.5
C5—C4—H4	109.5	N1—C13—H13B	109.5
C3—C4—H4	109.5	H13A—C13—H13B	109.5
C5—O5—H5O	111 (2)	N1—C13—H13C	109.5
O5—C5—C6	108.62 (17)	H13A—C13—H13C	109.5
O5—C5—C4	108.92 (15)	H13B—C13—H13C	109.5
C6—C5—C4	112.72 (16)	O10—C14—H14A	109.5
O5—C5—H5	108.8	O10—C14—H14B	109.5
C6—C5—H5	108.8	H14A—C14—H14B	109.5
C4—C5—H5	108.8	O10—C14—H14C	109.5
C6—O6—H6O	110 (2)	H14A—C14—H14C	109.5
O6—C6—C5	113.26 (17)	H14B—C14—H14C	109.5
O6—C6—H6A	108.9		

C7—N1—C1—C2	75.2 (2)	C4—C5—C6—O6	55.7 (2)
C13—N1—C1—C2	−75.3 (2)	C1—N1—C7—C8	24.6 (3)
N1—C1—C2—O2	11.7 (3)	C13—N1—C7—C8	174.25 (19)
N1—C1—C2—C3	−169.53 (16)	C1—N1—C7—C12	−160.0 (2)
O2—C2—C3—O3	−7.0 (3)	C13—N1—C7—C12	−10.3 (3)
C1—C2—C3—O3	174.20 (16)	C12—C7—C8—C9	−1.6 (3)

O2—C2—C3—C4	117.2 (2)	N1—C7—C8—C9	174.0 (2)
C1—C2—C3—C4	−61.6 (2)	C7—C8—C9—C10	0.5 (4)
O3—C3—C4—O4	70.7 (2)	C8—C9—C10—C11	0.8 (4)
C2—C3—C4—O4	−53.0 (2)	C8—C9—C10—O10	−179.7 (2)
O3—C3—C4—C5	−48.3 (2)	C14—O10—C10—C9	3.2 (3)
C2—C3—C4—C5	−172.04 (16)	C14—O10—C10—C11	−177.2 (2)
O4—C4—C5—O5	180.00 (15)	C9—C10—C11—C12	−1.0 (4)
C3—C4—C5—O5	−60.6 (2)	O10—C10—C11—C12	179.5 (2)
O4—C4—C5—C6	59.4 (2)	C10—C11—C12—C7	−0.1 (4)
C3—C4—C5—C6	178.77 (18)	C8—C7—C12—C11	1.4 (3)
O5—C5—C6—O6	−65.1 (2)	N1—C7—C12—C11	−174.2 (2)

Hydrogen-bond geometry (Å, º)

D—H···*A*	*D*—H	H···*A*	*D*···*A*	*D*—H···*A*
O3—H3*O*···O4	0.87 (3)	2.67 (3)	2.962 (2)	101 (3)
O3—H3*O*···O5^{i}	0.87 (3)	1.94 (3)	2.747 (2)	153 (2)
O4—H4*O*···O6^{ii}	0.80 (3)	1.90 (3)	2.700 (2)	176 (3)
O5—H5*O*···O3^{iii}	0.86 (3)	1.86 (3)	2.702 (2)	165 (3)
O6—H6*O*···O5	0.82 (3)	2.56 (3)	2.918 (2)	108 (3)
O6—H6*O*···O4^{iv}	0.82 (3)	1.95 (3)	2.704 (2)	154 (3)

Symmetry codes: (i) *x*, *y*+1, *z*; (ii) −*x*, *y*+1/2, −*z*+2; (iii) −*x*+1, *y*−1/2, −*z*+2; (iv) *x*, *y*−1, *z*.

Supplementary Table S1. Chemical shifts (ppm) of peaks for selected carbon atoms in a ^{13}C NMR spectrum of (I) in D_2O/pyridine (1:1) at 293 K and in the solid state

Carbon	*α*-pyranose	*β*-pyranose	*α*-furanose	*β*-furanose	acyclic *keto*	solid state
C1	60.97	63.21	61.28	61.28	62.41	57.23
C2	101.13	101.56	108.26	105.62	215.08	210.04
C3	73.62	71.99	84.62	79.73	78.93	77.80
C4	74.92	72.98	80.26	77.42	74.96	69.59
C5	66.66	71.99	85.64	83.77	73.45	69.59
C6	63.7	65.90	64.37	65.14	65.81	64.70
C13	n.r.	42.62	n.r.	42.09	41.85	39.56